Investigation of the co-crystallisation of N-heterocycles

By

Leigh-Anne Loots

Thesis presented in partial fulfilment of the requirements for the degree of Master of Science

at

Stellenbosch University

Department of Chemistry and Polymer Science

Faculty of Science

Supervisor: Leonard J. Barbour

March 2009

Declaration

By submitting this thesis electronically, I declare that the entirety of the work contained therein is my own, original work, that I am the owner of the copyright thereof (unless to the extent explicitly otherwise stated) and that I have not previously in its entirety or in part submitted it for obtaining any qualification.

March 2009

Acknowledgements

- Firstly, I would like to thank my supervisor Prof. Len Barbour for giving me the opportunity and freedom to explore the field of supramolecular chemistry. I am very grateful for the opportunities I have been given to broaden my scientific knowledge in the lab as well as abroad. I appreciate your advice, insight and guidance

- Dr Jan-André Gertenbach for his advice and guidance during my studies. For helpful discussions and ideas throughout and for his never-ending encouragement and enthusiasm for my project

- Dr Catharine Esterhuysen for the theoretical calculations performed on selected structures.

- Drs Regine Herbst-Irmer and Ina Dix for their help in refining the twinned structure *β*–O2N2.

- Jean McKenzie and Elsa Malherbe for NMR spectra.

- Dr Delia Haynes for her open door policy for random discussions

- The Supramolecular Materials Chemistry Group members, past and present, at the University of Stellenbosch, who have created a friendly working environment in which to learn and grow as a researcher. Members of the extended group include Prof. Len Barbour, Dr Martin Bredenkamp, Dr Catharine Esterhuysen, Dr Jan-André Gertenbach, Dr Delia Haynes, Dr Tanya Le Roex, Dr Dinabandu Das, Dr Subhadip Neogi, Dr Liliana Dobrzańska, (soon to be Dr) Tia Jacobs, Charl Marais, Bettinah Chipimpi, Marlene Milani, and Eustina Batisai and, last but far from least, my close friend Storm Potts.

- My dear friends and family who have been patient, understanding and supportive throughout. I love and cherish you all.

- The National Research Foundation (NRF) for financial support

LIST OF ABBREVIATIONS

ASU	–	Asymmetric Unit
SCD	–	Single Crystal X-ray Diffraction
PXRD	–	Powder X-ray Diffraction
DSC	–	Differential Scanning Calorimetry
API	–	Active Pharmaceutical Ingredient
CA	–	Co-crystallising agent
GRAS	–	Generally Regarded As Safe
FDA	–	Food and Drug Administration
CSD	–	Cambridge Structural Database
SDG	–	Solvent–Drop Grinding
NMR	–	Nuclear Magnetic Resonance
MAS-NMR	–	Magic Angle Spinning Nuclear Magnetic Resonance
CPK	–	Corey, Pauling and Koltun
δ	–	Chemical Shift (in ppm)
IR	–	Infrared
CIF	–	Crystallographic Information File
T_{on}	–	Onset Temperature
M_r	–	Molecular mass
mp	–	melting point
Z	–	Number of formula units in the unit cell
α	–	angle between the *b* and *c* axes
β	–	angle between the *a* and *c* axes
γ	–	angle between the *a* and *b* axes
θ	–	angle of X-ray incident beam or angle between D–H⋯A in hydrogen bond
ρ	–	density
1-D	–	One Dimensional
2-D	–	Two Dimensional
3-D	–	Three Dimensional
N_{arom}	–	Aromatic Nitrogen
C_{arom}	–	Aromatic Carbon

CONFERENCES

ECM ’07 – *24 European Crystallographic Meeting*

Marrakech Morocco, 22-27 August 2007

Poster presentation – *Do polymorphs have a predilection for forming co-crystals?*

ICMR 2008 – *International Centre for Materials Research Summer School on Periodic Structures and Crystal Chemistry*

University of California Santa Barbara, July 27 – August 9 2008

Poster presentation – *Motif Mimicry in Hydroquinone Co-crystals*

SACI 2008 – 39th *National Convention of the South African Chemical Institute*

Stellenbosch, South Africa, 30 November – 5 December 2008

Poster Presentation – *Motif Mimicry in Hydroquinone Co-crystals*

PUBLICATIONS (not part of this work)

Weber, W. G.; McLeary, J. B.; Gertenbach, J. A.; Loots, L., Dibenzyl pentathiodicarbonate. *Acta Crystallogr. Sect. E,* **2008,** 64, O250.

Abstract

Co-crystals are excellent materials for studying intermolecular interactions in the solid-state and can be used to further our knowledge of the balance between strong and weak intermolecular interactions. The O–H$\cdots$N$_{arom}$ synthon was chosen as the focus of this investigation of hydrogen bonding motifs. The starting materials selected all have two hydrogen bond donor and/or acceptor sites for the formation of extended networks. All molecules are also aromatic such that the influence of weaker $\pi\cdots\pi$ interactions can be included in the study. Two 3×3 grids of related co-crystals were produced from these starting materials and are reported in this thesis as part of an ongoing investigation into a broader set of co-crystals.

A part of the work describes the investigation of co-crystals prepared by the combination of related benzenediol and diazine isomers taken from a 3×3 grid. The solid-state structures of each of the six starting materials are discussed briefly to describe the nature of intermolecular interactions involved in the single component crystals. Trends in hydrogen-bonding patterns as well as the weaker interactions identified in the starting materials, can be used to recognise those in the subsequent multi-component crystals. Thirteen co-crystal compounds were obtained, of which twelve structures are novel. Each of these co-crystal structures is discussed in terms of intermolecular interactions and packing in the solid state. Hydrogen-bonding patterns and structural similarities are highlighted in related co-crystal structures as well as between co-crystals and their respective starting materials.

The combination of benzenediol isomers with benzodiazine isomers yielded seven novel co-crystal structures in a second 3×3 grid is reported. The structure of phthalazine, which has not yet been reported, is included in addition to these co-crystals, while the structures of quinazoline and quinoxaline that were retrieved from the CSD are discussed briefly. Co-crystal structures are discussed individually, focusing on the intermolecular interactions that are significant to the structural architecture of the compound. Certain co-crystals that display structural similarities with structures of the 3×3 grid, as well as with co-crystals presented in Chapter 3, are discussed in the relevant sections.

Lastly, two extended pyridyl diyne ligands that were synthesised for use in future co-crystallisation studies similar to those reported earlier are briefly highlighted. The crystal structures of the pure compounds and of a hydrate of one of the ligands were obtained and discussed briefly. To date only one of these structures has been reported in the literature.

Opsomming

Mede-kristalle (co-crystals) is uitstekende materiale vir die studie van intermolekulêre interaksies in die vastetoestand en kan gebruik word om die kennis van die balans tussen sterk en swak intermolekulêre interaksies te verbreed. Die O–H$\cdots$N$_{arom}$ sinton is gekies as die fokus van hierdie navorsing van waterstofbindings motiewe. Die geselekteerde uitgangstowwe het almal twee waterstofbinding donor en/of akseptor posisies vir die formasie van uitgebreide netwerke. Alle molekules is ook aromaties sodat die invloed van swakker $\pi\cdots\pi$ interaksies ingesluit kan word. Twee 3×3 stel van verwante mede-kristalle is voorberei vanaf hierdie reagense en word gerapporteer in hierdie tesis as deel van ’n langdurige studie van ’n groter stelsel mede-kristalle.

’n Gedeelte van die werk beskryf ’n ondersoek van mede-kristalle wat uit ’n kombinasie van verwante benseendiol en diasien isomere berei is om ’n 3×3 stel te maak. Die vastetoestand strukture van elk van die ses reagense is kortliks bespreek om die aard van intermolekulêre interaksies betrokke in die enkel-komponent kristalle te verduidelik. Tendense in patrone van waterstofbindings, sowel as dié van swakker interaksies kon geidentifiseer word deur die vastetoestandstrukture van die uitgangstowwe en uiteindelike multi-komponent kristalle te vergelyk. Dertien mede-kristalle is verkry waarvan twaalf nuwe strukture is. Elkeen van hierdie dertien mede-kristal strukture is beskryf in terme van intermolekulêre interaksies en die rangskikking in die vastetoestand. Waterstof-bindings patrone en verwantskappe tussen strukture is uitgelig in verwante mede-kristal strukture asook tussen mede-kristalle en hul afsonderlike uitgangstowwe.

Die kombinasies van benseendiol isomere en bensodiasien isomere lewer sewe nuwe mede-kristalstrukture in ’n tweede 3×3 stel. Die struktuur van ftaalasien, wat nog nie in die literatuur gerapporteer is nie, is ingesluit saam met die mede-kristalle, terwyl die kinasolien en kinoksalien strukture wat vanaf die CSD verkry is kortliks beskryf word. Die mede-kristal strukure is individueel bespreek, en daar word gefokus op die intermolekulêre interaksies wat belangrik is vir die strukturele argitektuur van die verbindings. Sommige van die mede-kristalle vertoon strukturele ooreenkomste met ander kristalle in die stel, asook met die voriges en word in toepaslike afdelings bespreek.

Laastens, twee uitgerekte pyridyl diyne ligande wat gesintetiseer word uitgelig vir vir die gebruik in toekomstig mede-kristallisasie studies soortgelyk aan die reeds genoem. Die kristalstrukture van die suiwer verbindings en ’n hidraat van een van die ligande is verkry en word kortliks beskryf. Net een van hierdie strukture is al in die literatuur gerapporteer.

TABLE OF CONTENTS

CHAPTER 1 – Introduction

CHAPTER 2 – Experimental Techniques

CHAPTER 3 – Co-crystals of benzenediol and diazine isomers

CHAPTER 4 – Co-crystals of benzenediol and benzodiazine isomers

CHAPTER 5 – Synthesised ligands and future studies

CHAPTER 6 – Summary and Concluding Remarks

APPENDICES

List of Figures

List of Tables

List of Schemes:

Atom Colours

Carbon

Oxygen

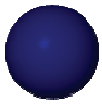

Nitrogen

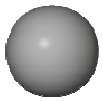

Hydrogen

CHAPTER 1

Introduction

"There is no more basic enterprise in chemistry than the determination of the geometrical structure of a molecule. Such a determination, when it is well done, ends all speculation as to the structure and provides us with the starting point for the understanding of every physical, chemical and biological property of the molecule."[1]

R. Hoffman in Determination of the Geometrical Structure of Free Molecules, MIR Publishers: Moscow, 1983.

In most areas of chemistry, a crystal structure determination is seen as the pinnacle of the study – the end product confirming successful completion of a synthetic procedure. However, for supramolecular chemists it is merely the beginning.[2] In 1993, Aakeröy and Seddon stated, in reference to the structure of a crystal, that "*the structural information could be treated as the beginning of a new venture, leading to questions of far reaching and fundamental importance regarding the interrelationships between molecules and ions in the solid state*".[2] Crystal structures, in most circumstances, represent a freeze-frame of molecular interactions, bonding and non-bonding, thus yielding important information regarding subtle interactions to be disentangled and applied to the design of supramolecular materials *i.e.* crystal engineering.[2] A brief introduction to the concepts essential to the work is presented here, but it is by no means a complete review of these concepts.

1.1 SUPRAMOLECULAR CHEMISTRY

Supramolecular chemistry can be described as the investigation of the relationships between molecules rather than between atoms. According to Lehn "*supermolecules (crystals) are to molecules and the intermolecular bond what molecules are to the atom and covalent bond*."[3] The concept of chemistry 'beyond the molecule'[4] was first proposed by Pepinsky[5] and later by Schmidt.[6] The field of supramolecular chemistry is applicable to a diversity of disciplines, all seeking to create new materials or to understand biological processes. The diverse nature of these systems has led to contributions from, and consequently collaborations between, physicists, theoreticians and computational modellers, crystallographers, inorganic and solid-state chemists, synthetic organic chemists, biochemists and biologists.[1] Supramolecular chemistry thus provides a link between visual, computational and experimental chemistry.[7]

The widespread interest in supramolecular compounds is due to the functionality of many of these compounds. Functionality is thought to be derived from specific structural elements within the crystal structure. In order for specific functionality to be implemented in the

design of new materials, a fundamental knowledge of the contributing factors is required. These aspects include the structure of individual molecules (e.g. the relationship between conjugation and colour of organic molecules) or the mode of aggregation of these molecules in the solid-state (e.g. polar ordering for conduction). One of the major objectives of the supramolecular chemist, at least during the early stages of the field, was to establish the characteristic forces responsible for the organisation of molecules in the solid state and to investigate how these forces can be manipulated and exploited. The accumulation and implementation of this information to construct solid-state materials is referred to as "crystal engineering".

Supramolecular systems that have been examined extensively include the inclusion compounds (host:guest systems) subdivided into clathrates,[8] rotaxanes,[9] calixarenes,[10] cyclodextrins[11] and cryptands.[1] Inclusion compounds are typically comprised of a 'host' framework (organic molecules, in most instances) that encapsulates a smaller 'guest' molecule. Other supramolecular species that are highly topical include metal-organic frameworks (MOFs)[8-10], zeolite-like metal-organic frameworks (ZMOFs)[12] and zeolitic imidazolate frameworks (ZIFs)[13,14] – these are especially important in the area of gas storage and separation. Co-crystal compounds[15-18] and polymorphism are supramolecular phenomena of special interest to the pharmaceutical industry.

"Engineering implies function-oriented design of the superstructure, selection of the building blocks…,their assembly and characterisation, to end with evaluation of the properties of the resulting supramolecular aggregate."[15]

Braga and Grepioni

1.2 CRYSTAL ENGINEERING

Crystal engineering as a scientific discipline is still in its infancy but is rapidly becoming one of the most intriguing, versatile and sought-after approaches to materials design. The foundation of crystal engineering is in the concepts of molecular recognition and self-organisation. Recognition events between complementary molecular fragments gives rise to the organisation of molecules in the solid state.[2] The recognition process relies on a number of factors for the assembly of a solid-state structure, including hydrogen bonding between molecular functional groups, complementary geometry of molecules i.e. (humps fit into bumps) and other directing factors (*e.g.* $\pi\cdots\pi$ interactions). Self-organisation is the basis upon which complex matter is formed and mechanisms are generally complex. Structures

that 'self-organise' can be designed to do so by selecting suitable components and interactions for supramolecular synthesis, and is considered self-organisation by design.

Owing to their directional characteristics and structural consequences, intermolecular interactions are the cornerstone of crystal engineering with the potential of controlling assembly of molecular building blocks into infinite architectures.[7] Crystal engineering then encompasses an "*understanding of intermolecular interactions in the context of crystal packing and in the utilisation of such understanding in the design of new solids with desired physical and chemical properties*".[16]

Statistical analysis of structures retrieved from databases, combined with *ab initio* investigations, is a prerequisite for examining intermolecular interactions. Data collected from such investigations are subsequently implemented in the synthesis of new functional compounds.[7] Since crystal structures are built from a delicate balance of these interactions, an understanding of their strength and directionality, and subsequent control, is of vital importance.[7]

It is recognised that recurring patterns often occur between molecules in the solid-state. These patterns can be used as building blocks that assemble *via* recognition between molecular fragments. Assembling a collection of robust building blocks (supramolecular synthons, Section 1.4) that interact in a specific, reliable and reproducible manner,[3] is expected to contribute to the predicable organisation of molecules into supramolecular systems. Functionality of these materials could then be tailored by modification of the building blocks. The formulation of a hierarchy of these building blocks would constitute a substantial increase in control over the 'self-organisation' of these systems.

1.3 INTERMOLECULAR INTERACTIONS

Intermolecular interactions are regarded as the communication network between molecules, and are responsible for the organisation of these molecules into an ordered arrangement to make up the "supermolecule" or crystal. Typically, intermolecular interactions are either medium- or long-range. Medium-range forces are of an isotropic nature and influence molecular shape, size and close-packing.[17] Examples include C⋯H, C⋯C and H⋯H interactions. Long-range interactions, on the other hand, are electrostatic and highly directional, taking place between heteroatoms such as N, O, S, Cl, Br, I or between these atoms and C or H.[17] The most prominent of these long-range forces in the solid-state is the hydrogen bond, which is discussed in more detail below, along with a number of other important interactions involved in the structures of this study.

"The strong hydrogen bond is the master-key of molecular recognition, and full control of this interaction will lead to mastery of supramolecular chemistry in general."[18]

Gautam R. Desiraju

1.3.1 HYDROGEN BONDING

The directing nature of the hydrogen bond in the solid-state brings with it control over physical processes apparent in the crystalline form such as optical properties, thermal stability, solubility, colour, conductivity, crystal habit and mechanical strength.[2] The frequent occurrence, along with the strength and directional nature of the hydrogen bond, make it a robust and specific interaction in the supramolecular context.[18]

The hydrogen bond is arguably regarded as the most important interaction in supramolecular chemistry and it is also ubiquitous in biological systems (DNA, protein-binding, *etc*). Its versatility is conferred by an energy contribution between that of covalent and van der Waals forces,[19] making it available for reversible reactions. These are especially important in biological systems.

Hydrogen bonding is divided into three main categories: very strong, strong and weak, according to strength and directionality (Table 1.1). The intermolecular forces involved, namely covalent, electrostatic and dispersion forces, influence the strength and directionality of the bond.[20] There have been numerous studies on hydrogen bonding providing an abundance of information on the subject.[15,18-21]

The geometry of a typical hydrogen bond between a donor atom (D) and an acceptor atom (A), related by an angle θ, is shown in Scheme 1.1.

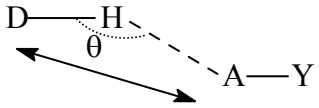

Scheme 1.1 Definition of the hydrogen bond of the type D–H····A–Y.[18]

The simple two centred D–H····Y hydrogen bond, as shown in Scheme 1.1, tends towards linearity with θ values in the range 150-180°.[17] Contact distances less than the sum of the van der Waals radii of the interacting atoms D and A, and θ angles that are near linear, are characteristic of strong hydrogen bonds.[15]

Table 1.1: Some properties of strong, moderate, and weak hydrogen bonds; adapted from a table in "The Weak Hydrogen Bond in Structural Chemistry and Biology."[19] The numerical data are guiding values only.[20]

	Very Strong	**Strong**	**Weak**
Interaction type	Strongly covalent	Mostly electrostatic	Electrostatic / dispersive
Bond Energy / -kcal mol^{-1}	15-40	4-15	<4
Examples	$[F\cdots H\cdots F]^-$	O－H····O＝C	C－H····O
	$[N\cdots H\cdots N]^+$	O－H····O－H	O－H····π
Bond lengths / Å			
H····A	1.2–1.5	1.5–2.2	2.0–3.0
Lengthening of D－H / Å	0.08–0.25	0.02–0.08	<0.02
D－H versus H····A	D－H ≈ H····A	D－H < H····A	D－H « H····A
D····A / Å	2.2-2.5	2.5-3.2	3.0 –4.0
Bonds shorter than van der Waals radii	100%	Almost 100%	30-80%
directionality	Strong	moderate	Weak
Bond angles, θ /°	170-180	>130	>90
Effect on crystal packing	Strong	Distinctive	Variable
Utility in crystal engineering	Unknown	Useful	Partly useful

A broad definition of hydrogen bonds proposed by Pimentel and McClellen (1960) makes no assumptions about the nature of the bonding atoms and therefore includes borderline donors and acceptors.[19] Pauling provided a more expansive definition in a chapter on hydrogen bonding found in *The nature of the chemical bond* stating that "*under certain conditions an atom of hydrogen is attracted by rather strong forces to two atoms, instead of only one, so that it may be considered to be acting as a bond between them*".[19] He implemented a further restriction, stating that a hydrogen bond can only form between electronegative atoms as the interaction is electrostatic in nature.[19] However, the most accepted definition of a hydrogen bond is that '*a hydrogen bond exists where there is evidence that it exists*'.[2]

Under normal circumstances, the location of an atom is based on the centres of gravity of the nucleus and its electron shell, which are in good agreement.[20] Because the hydrogen atom consists of only a single electron, paired with the nucleus, the exact location of the atom becomes difficult to assign accurately.[20] This is because, when bonded to electronegative atoms by covalent interactions, the average position of the hydrogen electron is skewed towards the more electronegative atom and so the centres of gravity of the nucleus and electron no longer coincide.[20] Where, then, is the hydrogen atom located? A

combination of neutron and X-ray diffraction analysis provides the most accurate positional data. Neutron diffraction locates the position of the nuclei, while X-ray diffraction determines electron-density maxima of the atoms.[20] Despite neutron diffraction being the more accurate technique for locating atomic nuclei, X-ray diffraction is more widely accessible for routine structure determination. For hydrogen positions located by X-ray diffraction to be considered acceptable, the D–H bond is generally "normalised". This is achieved by relocating the hydrogen atom (electron centre of gravity) along the D–H vector to a position corresponding to an averaged internuclear distance (approximate proton position) determined by neutron diffraction.[20] Standard bond lengths (in Å) currently in use are O–H = 0.983, N–H = 1.009, C–H = 1.083[20] and C_{arom}–H = 0.950 For the purposes of this study, focus is placed on the D⋯A distance of the hydrogen bond, as it is more accurately determined, although reasonable D–A distances have been included for completeness.

The utility of the hydrogen bond stems from its long-range character, which is important in the organisation of molecules into predictable arrays.[19] It has been argued that these interactions are felt by molecules as they approach one another, prior to nucleation in the solution-state, before dispersive interactions determining close-packing and stabilization energies are felt.[19] Desiraju and Steiner summarise the influence of the hydrogen bond in the solid-state, in their book *The Weak Hydrogen Bond in Structural Chemistry and Biology*, with the following statement "*the hydrogen bonds (weak and strong) determine the general connectivity patterns of molecules, while the isotropic interactions determine both intramolecular conformations and intermolecular close-packing within the basic scaffolding established by the hydrogen bonds.*"

It is generally accepted that the stronger hydrogen bonds are key in effectively controlling the crystal and supramolecular structure of a molecule. These include O—H⋯O=C, N—H⋯O=C and O—H⋯O—H bond types.[19] In contrast, weak interactions are involved to a lesser extent and their influence on the packing arrangement of the crystal structure can vary. This is due to the electrostatic nature of the bond that is modified by variable dispersive and charge-transfer contributions that are dependent on the donor and acceptor atoms.[19] Examples of weak interactions are O—H⋯Ph and C≡C—H⋯O types.[19] The majority of strong hydrogen bonds observed during this study are the O–H⋯N and, to a lesser extent, O–H⋯O bonds. Typical D⋯A distances of the O–H⋯N interaction, determined by a CSD survey, occur in the range 2.60–2.90 Å with θ angles of 150–180°. These parameters are comparable to those of O–H⋯O interactions.

Weakly directional hydrogen bonds are difficult to describe in terms of their impact on the packing of a crystal structure as they are often overshadowed by much stronger interactions. The weak hydrogen bond is differentiated from strong hydrogen bonds by the moderate to low electronegativity of the donor and/or acceptor atoms.[19] Interactions of this type influence the crystal structure to varying degrees, of which three roles are apparent – innocuous, supportive or intrusive. Innocuous bonds have little impact on the structure, supportive bonds are congruent with the orientation requirements of other interactions in the structure, and weak hydrogen bonds that appear to steer packing are regarded as intrusive.[19]

The C–H⋯(O,N) type interactions are arguably the most important of the weakly directional forces in a range of chemical and biological systems.[17] C⋯O contact distances of between 3.0–4.0 Å are typical of these interactions, with θ angles ranging from 100–180° with an increased frequency between 150–180°.[17] The reciprocal (O,N)–H⋯C are uncommon owing to the electropositive nature of the carbon atom as well as steric hinderance for most sp^3 hybridised atoms.[17] For a carbon atom to act as a hydrogen bond acceptor it requires additional electronegativity, which can be supplied in the form of unsaturated C–C bonds such as alkynes, alkenes and aromatic rings in which electrons are delocalised over the contributing atoms.[17]

1.3.2 CLOSE PACKING

Kitaigorodskii has suggested that the phenomenon of close packing is "*the manifestation of the maximisation of favourable isotropic van der Waals interactions*".[1,22] In essence, molecules tend to pack efficiently, occupying all available space, while maximising energetically favourable van der Waals contacts.[22] A simplification of the principle is that humps fit into bumps, much like the '*lock and key principle*' in biological enzymatic systems. The fulfilment of close-packing within a crystal structure mostly results in the utilisation of only a small number of space groups, namely $P2_1/c$, $P\bar{1}$, $C2/c$, $P2_1$ and $P2_12_12_1$.[23]

1.3.3 π－ACCEPTORS

Acceptors of this type are generated by moieties such as alkenes (C＝C), alkynes (C≡C) and, in most instances, aromatic rings. Here focus is placed on the aromatic type acceptors as they are more established and exhibit specific interaction motifs. Aromatic entities have the capacity to interact with one another in two common orientations, namely face-to-face (stacking interactions) and edge-to-face (also known as T-shaped) (Figure 1.1). The face-to-

face conformation or π·····π stacking can be eclipsed or offset (also referred to as slipped π-stacks or skewed stacks).[24] A similar charge of electron clouds, in close proximity, is compensated for by adopting the offset conformation and is preferential for identical interacting molecules.[25] Eclipsed face-to-face stacking appears to be more favourable if the participating molecules are dissimilar and/or have complementary electron distributions.

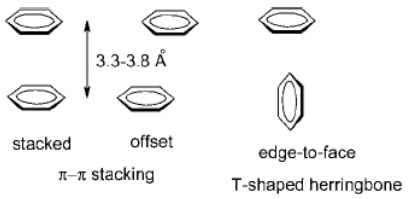

Figure 1.1 The different types of π·····π interactions found between aromatic rings.[30]

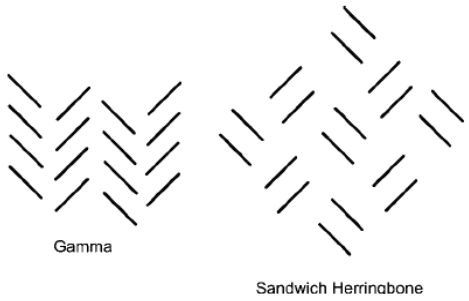

Figure 1.2 Two typical herringbone packing types – Gamma and sandwich herringbone.[30]

Eclipsed face-to-face stacking yields a characteristic graphitic layering, whilst edge-to-face interactions can be credited for the familiar herringbone packing pattern (Figure 1.2, left) commonly found in the structures of small aromatic molecules.[1] Acceptable plane separation for the parallel stacked, and offset type stacking is approximately 3.3–3.8 Å.[26] Edge–to–face centroid–to–centroid distance can be as long as 5 Å.[24]

Geometrical criteria are also an important consideration when studying aromatic molecules in the solid state. Aromatic molecules are generally disc shaped, which lends to efficient stacking of the molecules but also creates intermolecular space surrounding the edges.[24] A factor determining the packing mode adopted by the molecules is the area of the aromatic ring compared to its thickness. Molecules with relatively small areas are likely to form edge–to–face interactions, that assemble in the crystal to form a herringbone pattern.[24] Offset interactions tend to be preferred with increasing area of the molecules. The sandwich herringbone motif is an intermediate between the gamma herringbone and offset patterns.[24]

Larger, fused aromatic hydrocarbons pack predominately as offset stacks combined with edge-to-face interactions, thus yielding herringbone motifs.[25] Stacking interactions are also applicable to heteroaromatic molecules, and especially polycyclic arenes where carbon is substituted by N, O, or S. However, in these cases, as the π systems increase in size, the offset pattern dominates over edge-to-face interactions.[24]

1.3.4 LONE-PAIR⋯π INTERACTIONS

The lone-pair⋯π interaction has only recently been accepted by some within the supramolecular community as a supramolecular interaction. This interaction appears to be most evident in bio-macromolecules where it was first identified by Egli and colleagues in a left-handed Z-DNA duplex,[27] while it has more recently been found to exist in small molecular host-guest systems and is reported to be energetically favourable.[27] The intermolecular contact distance between the electron-rich atom and any of the six atoms of a (hetero)aromatic ring is limited to <4 Å and the distance to the centroid of the ring also does not exceed 4 Å.[27]

1.4 THE SUPRAMOLECULAR SYNTHON

"Supramolecular synthons are structural units within supermolecules which can be formed and/or assembled by known or conceivable synthetic operations involving intermolecular interactions."[3] Care should be taken not to confuse synthons with the intermolecular interactions involved in synthon construction in a structure. An interaction utilises chemical recognition between components, whereas a synthon relies on both chemical and geometrical aspects of the interaction.[3] The intermolecular interaction forms an integral part of the synthon and, on occasion, the synthon and the interaction involved cannot be differentiated from one another. The OH⋯N_{arom} is an example of such an occurrence (Figure 1.3). Distinction is also made between a supramolecular synthon and the functional group of a molecule. The most basic difference here is in the type of bond utilized to assemble these entities – a functional group is covalently bonded (*e.g.* carboxylic acid, alcohol, amide), while a synthon is a hydrogen bonded motif constructed from complementary functional groups. Functional groups are often used in the creation of supramolecular synthons *via* intermolecular interactions.

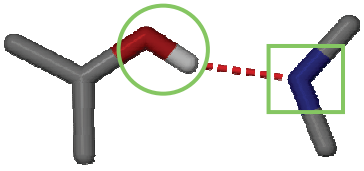

Figure 1.3 A supramolecular synthon OH⋯N_{arom} formed from the OH⋯N hydrogen bond. Functional groups are marked by the green circle (alcohol) and square (N_{arom}).

Two categories of supramolecular synthon exist – the homosynthon, formed from self-complementary donor and acceptor groups *e.g.* carboxylic acid dimer/catemer (***a***, Scheme

1.2), and the heterosynthon, comprised of different, yet complementary donor and acceptor groups (examples include acid–pyridine (***c***), hydroxyl–pyridine (***b***), acid–amide (***e***) *etc*.).[28] In order for heterosynthons to form, interactions must be more favourable than in the homosynthon.

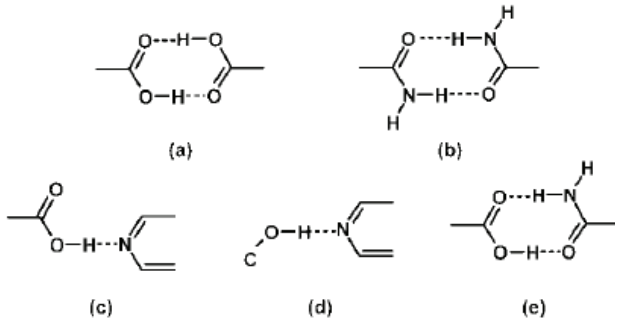

Scheme 1.2 Supramolecular homosynthons (a, b) and heterosynthons (c, d, and e). Figure taken from *Cryst. Growth Des*., 2008, **8**, 4533.[28]

1.5 CO-CRYSTALS

Co-crystals, although not considered to be a new class of supramolecular compounds (quinhydrone was first reported[29] in 1844), have only recently come to the forefront of supramolecular chemistry. However, the impact they have made in the CSD is still low, comprising only 1951 entries, ca. 1%, of all purely organic entries.[28] Co-crystals have garnered much controversy[30-32] over the past decade, both with regard to nomenclature and constitution. This raises the question: what is a co-crystal? All agree that a co-crystal is a "*multi-component molecular crystal*", *i.e.* a crystalline material comprising more than one component in the same lattice.[33] There is, however, discrepancy over the molecular components since the term "multi-component molecular crystals" encompasses a number of molecular assemblies, *viz.* solvates, hydrates, clathrates, inclusion compounds, *etc*. It is generally accepted that a co-crystal should consist of neutral molecules. A number of researchers[14,34,35] have imposed further restrictions, limiting starting materials to compounds that are solid under ambient conditions. This limitation has led to disagreement concerning classification of multi-component molecular crystals *not* prepared from solid materials. How a crystal prepared from a solid and a liquid or a liquid–liquid combination is categorised remains to be addressed and it is the opinion of the author that the states of the starting materials should be irrelevant when investigating the properties of the end product. It seems absurd to distinguish between "co-crystal" compounds based on physical composition of the starting materials, especially if these compounds are clearly part of a series of related compounds. Despite inconsistencies, the term "co-crystal" will most probably continue to be

used as a synonym for "multi-component molecular crystal" simply because it is more straightforward.[32]

Co-crystals can be prepared by many different crystallisation methods. Slow evaporation from solution is the method of choice, although grinding or solvent-assisted grinding (Section 1.8) techniques are gaining in popularity. Care should be taken when considering components since co-crystallisation is reliant on the resulting heteromeric species being more favourable than the homomeric form of either constituent.[2] The use of synthons in this regard has received widespread success.[2] Etter[34] established a set of guidelines for the effective combination of co-crystal components (synthons) into a somewhat predictable array. The most significant of these observations is that "*all good proton donors and acceptors are used in hydrogen bonding e.g. phenols, carboxylic acids, amides, imides, etc*." The hydrogen bonds then form in a hierarchical fashion, with the best-donor bonding to the best-acceptor then the second best-donor to the second best-acceptor and so on.[34] Further elucidation of a hierarchy of these synthons in a competitive environment would be instrumental in co-crystal engineering and *vice versa*. Co-crystals are ideally suited for investigating synthons in a competitive environment owing to their modular nature, and by definition, must be composed of two (or more) components.[28] Investigations of this nature are already under way.[6,37]

Etter and co-workers were the first to introduce the use of co-crystals as a means of studying packing patterns, hydrogen-bond motifs and intermolecular forces, and they also established a classification system used to describe these patterns.[7] This classification is known as Graph Set Notation and is discussed further in Section 1.7.

Co-crystals have become an area of wide interest in terms of the fundamental aspects of molecular-recognition-driven assembly processes[35] as well as applications in areas of host–guest compounds, nonlinear optics (NLO), organic conductors, modifications of photographic films,[36] or coordination polymers.[28] However, the most active area of co-crystal research is that of pharmaceutical co-crystals.

1.5.1 PHARMCEUTICAL CO-CRYSTALS

Pharmaceutical co-crystals can be described as a subset of co-crystals that form between an active pharmaceutical ingredient (API) and a co-crystallising agent (CA) that are both solids under ambient conditions.[36] The propensity for APIs to form co-crystals is driven by the location of hydrogen bonding moieties on the exterior of the molecule that are thus accessible to co-crystal formers.[36] This characteristic has, in the past, been detrimental as

such molecules are inclined to form polymorphs as well as solvates or hydrates in an unpredictable manner. However, the use of co-crystal forms of APIs in pharmaceutical preparations has contributed increased stability as well as improved physicochemical properties of these APIs. Prior to co-crystal forms, APIs were limited to formation of salts, polymorphs, hydrates and solvates, each with their own obstacles.[37] The formation of novel API co-crystals is limited only by the number of co-crystal formers available. Currently there are hundreds of potential co-crystallising agents that comply with GRAS (Generally Regarded As Safe) regulations, including food additives, that remain to be tested.[36] Because the API is not covalently modified in the co-crystal form, it is anticipated that these new pharmaceutical co-crystals will afford forms of APIs with enhanced physical properties such as improved solubility, stability, hygroscopicity and dissolution rates.[36] The nature of the interactions between molecules in co-crystals also creates the potential for use in isolation or purification of APIs during processing, after which the CA is removed prior to formulation.[36]

Because co-crystals present the possibility for an increased number of API formulations, protection of intellectual property is an essential part of the scientific process. As with most industries, safeguarding of intellectual property (IP) is essential to a company's economic growth. Pharmaceutical companies are particularly dependent on meticulous IP protection owing to the nature of the industry – drug formulations undergo years of research and development, followed by rigorous testing and clinical trials, to ensure that all regulations are met before the product can eventually be marketed.[38] Patents are the means by which scientific and technological inventions are safeguard and there are three criteria that must be met for an invention to be considered patentable: novelty, utility and non-obviousness. Certainly, co-crystals easily fulfil the novelty criterion as new and distinct solid-state structures. The lack of patents involving co-crystals suggests that the field is poised for potentially novel co-crystal inventions.[38] The enhancement in solubility, dissolution rate profiles and consequently bioavailability of APIs in the co-crystal form has been shown to improve the therapeutic efficacy of the particular drug. This is evidence of the co-crystal's utility. The non-obvious criterion is often the most difficult to satisfy and is said to be analogous to predictability.[38] The solid-state structure of co-crystals is, at present, anything but predictable and a large component of research is focussed on the understanding of intermolecular interactions involved in the organisation of these molecules in the solid-state. Thus, co-crystals are, in general, non-obvious.

Carbamazepine (CBZ) is an important anti-epileptic drug that exemplifies the improvement in physicochemical properties when co-crystallised. Carbamazepine has to date

manifested as four anhydrous polymorphs, a dihydrate, an acetone solvate and two ammonium salts. The co-crystal preparation with saccharin exhibits superior stability compared to the existing single-component crystal forms, showing favourable dissolution and suspension stability as well as a favourable oral absorption profile when administered in dogs. A recent report in the media (2007),[33] disclosed the deaths of more than 4000 pets after food intake and was later found to be caused by a co-crystal of melamine and cyanuric acid. This co-crystal was found to be highly insoluble in water and resulted in acute renal failure. Both components are relatively non-toxic individually but toxic in co-crystal form at a concentration of 32 mg kg^{-1} body weight in cats. Both of these examples highlight the relevance of co-crystal studies in pharmaceutical formulations.

1.6 POLYMORPHISM

Mitscherlich (1822)[39-41] first recognised that chemical compounds can have more than one crystal structure. McCrone (1965) later defined polymorphism as "*a solid crystalline phase of a given compound resulting from the possibility of at least two different arrangements of the molecules of that compound in the solid state.*"[42]

Polymorphism can have both positive and negative implications, and the pharmaceutical industry will be used as an example. The discovery of a more stable form with superior physicochemical properties compared to the previous form(s) is an obvious advantage. However, polymorphs may be difficult to separate from one another. A bigger problem, still, is if one form is a sought-after drug component while another form may be highly toxic. The structural flexibility inferred by numerous polymorphic forms is an advantage when seeking suitable co-crystallising agents. Structural flexibility provides for multiple modes of self-organisation or self-assembly with other molecules.[41] Compounds adopting polymorphic forms also affect other areas of industry, including agrochemicals, explosives, dyes, pigments, flavours and confectionery products.[41] Polymorphs can be distinguished from one another by studying their individual SCD structures and powder diffractograms, along with DSC analysis, IR spectroscopy, microscopy and a number of other techniques.[23]

1.7 GRAPH SET NOTATION

Graph set notation (or analysis) of a crystal structure is used to simplify the description of hydrogen bonding patterns. The idea, conceptualised by Margaret Etter (1990),[34,43] is to designate all hydrogen bonding patterns into one of four simple motifs or a combination thereof. Hydrogen bonding motifs are classified as chains (C), rings (R), self bonded (S) (*i.e.*

intramolecular interactions) or discrete (D) (Figure 1.4).[1] These four designators (*G*) combined with the number of hydrogen bond donors (subscript, *d*), acceptors (superscript, *a*) and the total number of participants (degree, *n*) in the motif, are considered to give a comprehensive description, $G_d^a(n)$, of the pattern.[1] Similar hydrogen bonding patterns in a series of hydrogen bonded structures can be identified using this nomenclature. The general procedure in assigning graph set notation to a hydrogen bonded system is to first assign hydrogen bond *motifs* (consisting of only one type of hydrogen bond) followed by the higher order *arrays* that make up the *network*.[2] The combination of graph set notation with a knowledge of supramolecular synthons and functional group similarities can be used to construct complex architectures from simple hydrogen bonding networks.

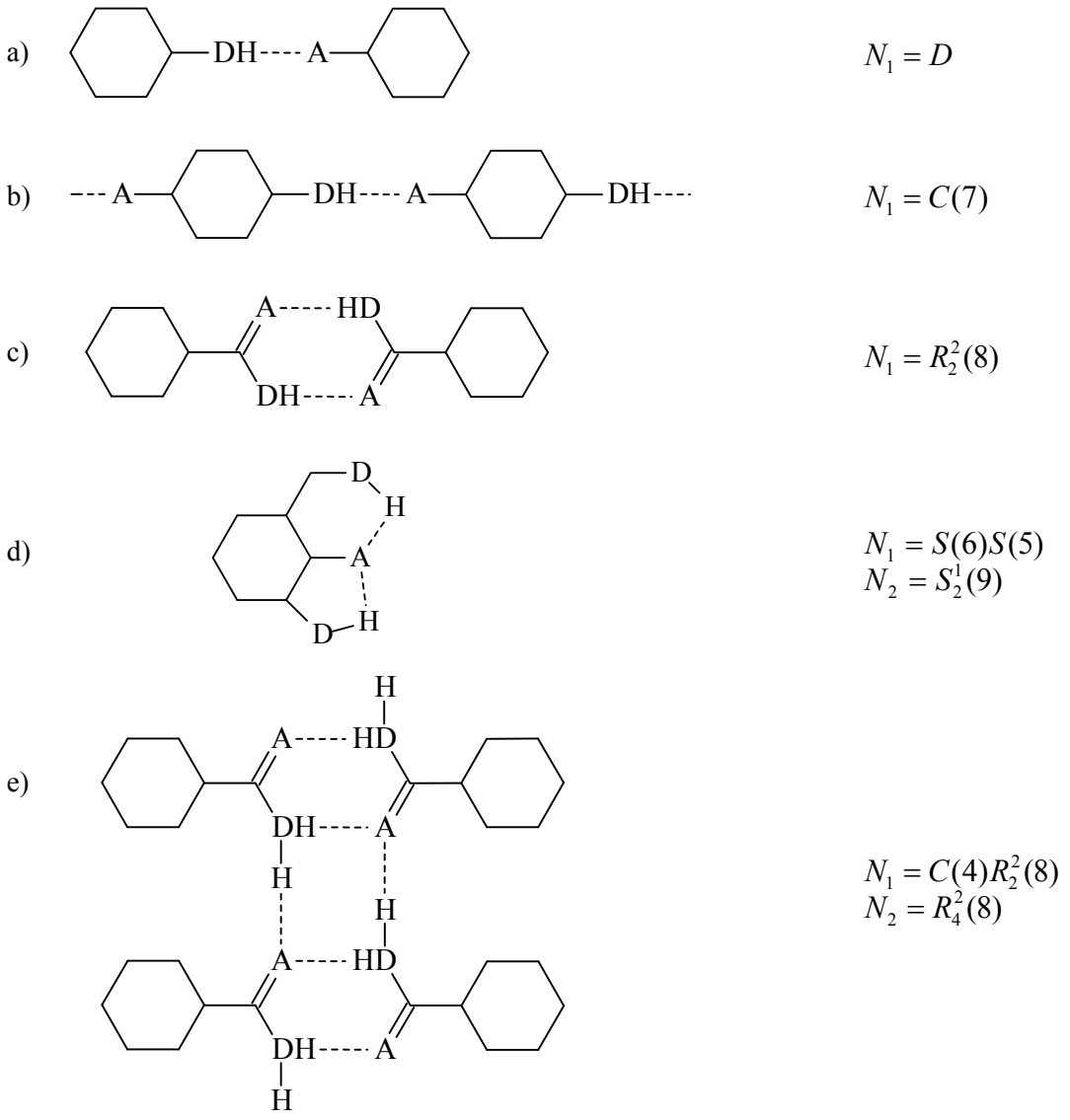

Figure 1.4 Examples of graph set assignments. The hexagons represent any organic ligand. Taken from *Acta Crystallogr., Sect. B* ,1990, **46**, 256-262.

1.8 SOLVENT DROP GRINDING (Solid-state reaction chemistry)

Crystalline products for X-ray diffraction studies can be obtained from slow evaporation of solvent,[44] vapour diffusion,[44] crystallisation from a melt, slurries[45,46] and solvothermal[47] methods, to name but a few.[48] Slow evaporation of solvent from a solution containing known molar quantities of co-crystal formers is the method of choice for co-crystallisations since it often yields single-crystals of suitable quality for SCD. As with any experimental technique, solvent evaporation has its drawbacks. It can be time-consuming waiting for crystals to grow, or establishing a suitable solvent system in which both components are soluble and, furthermore, starting materials may not be completely converted into the target product. In addition, the product may manifest in different forms (polymorphs) concomitantly or under different conditions.

In particular, grinding has come into regular use in investigations of co-crystals and salts. This technique involves pulverising two (or more) components together for a given period of time to yield a multi-component product. The grinding process is carried out either manually with a mortar and pestle, or mechanically with a mill. The physical benefit of grinding is a reduction in particle size, thus increasing the surface area available for reaction;[49] the mechanical energy put into the process generates enough heat to induce a number of solid-state transformations, including crystalline to amorphous, amorphous to crystalline, polymorphic conversion as well as solid-state reactions.[49]

A variation on the neat grinding method is solvent–assisted grinding, also referred to as solvent–drop grinding (SDG), which incorporates the use of a minimum of solvent (usually 3–5 drops). The addition of solvent supposedly increases the degrees of freedom of the molecules, enhancing the occurrence of molecular collisions. It can also act as a catalyst and possibly even provide tiny co-crystal seeds.[50]

The product of a grinding experiment is in general a micro-crystalline material that can be analysed by PXRD. It is, in some cases, possible to elucidate the single-crystal structure of this material *via ab initio*[48] calculations (Rietveld refinement) from PXRD results to yield a 3-D representation of the crystal structure. If this is not possible, the micro-crystals can be used to seed a saturated solution of the starting materials affording single crystals for SCD analysis. A PXRD pattern is then simulated from the crystal structure for comparison with the data obtained from the solvent-drop grinding experiment.

Mechanochemical preparation of co-crystalline material is particularly appealing as it can be incorporated into high-throughput synthesis of new materials, which can rapidly be screened by PXRD analysis. The speed with which these products can be produced and

analysed offers the potential of testing an increased number of variables, including temperature, concentration gradients, various solvent systems (polar, non-polar) and grinding duration.[51] In addition to these benefits, solvent-drop grinding is a cheaper, 'greener' and less time-consuming method of compound preparation.[48] However, other techniques should not be disregarded since, in some instances, solvent plays an important role in the arrangement of the molecules and the resultant crystal structure.

1.9 ASPECTS OF THIS STUDY

For the chemist not fully versed with the intricacies of co-crystals, the effort of bringing together different molecules into a single crystalline compound may seem trivial.[52] The complexities involved in bringing together two or more molecules without making or breaking covalent bonds while maintaining a level of control over intermolecular interactions, as well as the manner in which molecules are connected, is anything but trivial.[52] The formation of crystalline compounds involves a delicate balance between strong and weak intermolecular interactions as well as a measure of self-recognition and subsequent assembly of complementary molecules. Co-crystals offer the opportunity to investigate the intricacies of supramolecular interactions of organic compounds in a relatively controlled environment. Components can be selected from a variety of readily available compounds and/or novel molecules can be designed as required. The design of novel components provides the prospect of investigating specific aspects of the interactions in question. Focus has recently been placed on developing a hierarchy[28,53,54] of intermolecular interactions based on supramolecular synthons by placing them in competitive environments. The potential application of an established hierarchy is invaluable for the furthering of crystal engineering. Following this hierarchy, co-crystal components can be selected or designed such that binary, ternary and higher level compounds can be prepared with relative predictability, and thus impart a desired function to the final product.

The objective of this study is not to establish a hierarchy of synthons, but rather to determine the positional effects of donor and acceptor atoms about aromatic rings in the formation of hydrogen bonds in a relatively controlled environment. The data obtained from this type of study can be used to tailor the design of novel crystalline compounds in conjunction with the knowledge of synthon hierarchy. Apart from the design aspect, these data can be considered to be a contribution to the further understanding of these non-covalent forces in the solid-state.

The principle aim of this study is to prepare numerous co-crystals and investigate the intermolecular interactions concerned with the formation of these compounds. Nineteen novel co-crystal structures are reported here, and these are supplemented by data retrieved from the Cambridge Structural Database (CSD).

The opportunity to study a closely related group of compounds is provided by the relatively simple starting materials. The hydrogen bond donors (benzenediol isomers) are selected because of their structural flexibility and dual donor-acceptor character. Although, not all of these compounds have polymorphic forms, each of the hydroxyl hydrogen atoms of each molecule can be located in one of at least two positions. It has been found that the C_{ar}–O–H groups are predominantly co-planar with the aromatic rings of the molecule. A brief CSD survey revealed this to be the case in the majority of structures containing the aromatic hydroxyl group. Although it is assumed that this is because of the delocalised π-electrons of the ring that repel the hydrogen atom of the hydroxyl group, further investigation is required. The diazine molecules are known as an important class of molecules from which pharmacological compounds can be synthesised and the capacity to form co-crystals is advantageous with regard to the potential for forming products with improved physicochemical properties. The complementary diazine acceptor molecules are weakly basic compounds ideal for co-crystal formation. The monocyclic and bicyclic diazine molecules were selected as acceptors owing to their similarity in N–atom placement about their aromatic rings. This offers the opportunity to investigate the influence of increased molecular size on the arrangement of the crystal structure. A larger surface area in the benzodiazine molecules is expected to have increased space requirements, although an increased surface area lends to formation of stronger π⋯⋯π interactions. The chemical aspects of the interactions are not as apparent as the geometrical features. The chemical relationship between the two groups of acceptors is apparent in a comparison of basicity of the molecules. An almost identical trend is observed between the monocyclic and bicyclic diazine molecules (Table 1.2)[55] with basicity decreasing as N–atoms become more remote from one another *i.e.* the *ortho* configuration is more basic than *meta,* with *para* being least basic. Phthalazine (BN23) is the most basic acceptor molecule with a p*K*a value of 3.50. Adjacent N–atoms located in the 2,3-positions make BN23 more basic than the monocyclic N2, with N–atoms situated in the 1,2-positions. Both hydrogen bond donor and acceptor molecules utilised here have the capacity to take part in more than one hydrogen bond, allowing formation of extended hydrogen bonded networks.

Donor and acceptor molecules are combined with the intention of using the OH·····N_{arom} synthon. In this instance, the synthon is synonymous with the interaction between molecules. The alcohol moiety is the second most prominent functional group identified in the CSD after the ethers and is found in 33% of all prescription drugs (Table 1.3).[28] Indeed, 74% of the 25 035 molecular alcohol entries[28] retrieved from the CSD form heterosynthons with various acceptor groups. Of the 228 structures that contain alcohol and aromatic nitrogen atoms exclusively, 78% form the OH·····N_{arom} synthon.[28] This provides a sound foundation for co-crystallisation experiments using the OH·····N_{arom} synthon.

Table 1.2 The ε_{HOMO}, p*K*a and ionisation energy IE values of selected diazine molecules.[55]

Molecule	$-\varepsilon_{HOMO}/E_h$	p*K*a	IE/eV	Molecule	$-\varepsilon_{HOMO}/E_h$	p*K*a	IE/eV
N2	0.3797	2.33	10.41	**BN2**	0.3270	2.30	9.10
				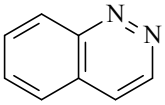			
				BN23	0.3317	3.50	9.07
				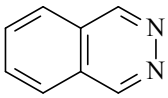			
N3	0.3752	1.30	10.61	**BN3**	0.3256	1.90	9.08
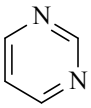				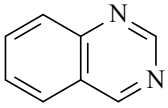			
N4	0.3588	0.70	10.18	**BN4**	0.3220	0.65	9.00
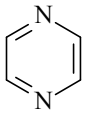				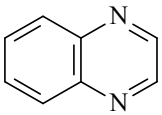			

Table 1.3 Cocrystal Design: % Occurrence of Functional Groups in APIs[a]. Table taken from T. R. Shattock, K. K. Arora, P. Vishweshwar and M. J. Zaworotko, *Cryst. Growth Des.*, 2008, **8**, 4533-4545. [28]

groups	CSD only organics	biological activity	pharmacological	prescription
ether	29	40	37	41
alcohol	21	39	36	**33**
ester	17	24	18	12
2° amide	9	18	22	14
carbonyl	14	22	16	28
2° amine	5	8	8	17
3° amine	7	12	13	43
C−Cl	9	13	16	21
$N_{aromatic}$	7	10	13	16
carboxylic acid	6	9	11	**25**
Cl-	3	8	9	16
sulfonamide	0.11	0.65	1.4	9

[a] CSD Conquest 1.10 (January 2008 update) 436 384 total entries. Search parameter: organics only 187 025 entries. Biological activity 11 046 entries, CSD All Text Search: Activity, Agent, Biological, Drug, Inhibitor, Pharmaceutical, Pharmacological.

The co-crystal compounds documented here were prepared either by slow evaporation of solvent or by a variation of solution seeding from material obtained *via* solvent-drop grinding. Single-crystal X-ray diffraction was used for structure elucidation with supplementary PXRD and DSC analyses. Hirshfeld surfaces, and fingerprint plots generated from these surfaces, provide an additional visualisation tool and theoretical calculations contribute to specific findings of relevant structures – α and β forms of O4N2 and the two scenarios of O4N3.

Discussion of the compounds prepared is structured into two main chapters (Chapters 3 and 4) according to the types of acceptor molecules used (diazine or benzodiazine). Structural elements are highlighted in each structure and similarities between compounds are discussed. A third chapter (Chapter 5) discusses compounds to be used in future co-crystal studies and the final chapter (Chapter 6) provides a summary of findings and a few general remarks regarding observations made during the study.

A note on nomenclature:

A systematic naming scheme for co-crystal compounds has not yet been established. Therefore, for the purposes of this study, an abbreviated system will be implemented. All starting materials are either *ortho (1,2)*, *meta (1,3)* or *para (1,4)* substituted phenol or pyridine molecules. Therefore, starting materials are named according to the type of substituents (O,N) and its position about the ring, using IUPAC nomenclature, i.e. catechol (1,**2**–benzenediol) will be **O2**, and pyrimidine (1,**3**-diazine) will be **N3**. The resulting co-crystal of catechol and pyrimidine is assigned **O2N3**. The benzodiazines will be named in a

similar manner, using the prefix **B** for benzo, to distinguish bicyclic rings from the monocyclic diazines, i.e. phthalazine (**2**,**3**–benzodiazine) will be BN**23**. When two forms exist, with different molar ratios, they will arbitrarily be assigned ***α*** and ***β***.

REFERENCES

1. J. W. Steed and J. L. Atwood, *Supramolecular Chemistry*, John Wiley & Sons, Ltd, 2000.
2. C. B. Aakeröy and K. R. Seddon, *Chem. Soc. Rev.*, 1993, **22**, 397-407.
3. G. R. Desiraju, *Angew. Chem., Int. Ed., Eng*, 1995, **34**, 2311-2327.
4. J.-M. Lehn, *Angew. Chem., Int. Ed., Engl.*, 1988, **27**, 89.
5. R. Pepinsky, *Phys. Rev.*, 1955, **100**, 971.
6. G. M. Schmidt, *J. Pure Appl. Chem*, 1971, **27**, 647-678.
7. C. B. Aakeröy, *Acta Crystallogr., Sect. B.*, 1997, **53**, 569-586.
8. J. E. D. Davies, *J. Incl. Phenom.*, 1998, **32**, 499-504.
9. J.-F. Moulin, J. C. Kengne, R. Kshirsagar, M. Cavallini, F. Biscarini, S. Léon, F. Zerbetto, G. Bottari and D. A. Leigh, *J. Am. Chem. Soc.*, 2006, **128**, 526-532.
10. P. K. Thallapally, G. O. Lloyd, J. L. Atwood and L. J. Barbour, *Angew. Chem., Int. Ed.*, 2005, **44**, 3848-3851.
11. G. Wenz, *Angew. Chem., Int. Ed.*, 1994, **33**, 803-822.
12. M. H. Alkordi, Y. Liu, R. W. Larsen, J. F. Eubank and M. Eddaoudi, *J. Am. Chem. Soc.*, 2008, **130**, 12639-12641.
13. W. Morris, C. J. Doonan, H. Furukawa, R. Banerjee and O. M. Yaghi, *J. Am. Chem. Soc.*, 2008, **130**, 12626-12627.
14. R. Banerjee, A. Phan, B. Wang, C. Knobler, H. Furukawa, M. O'Keeffe and O. M. Yaghi, *Science*, 2008, **319**, 939.
15. D. Braga and F. Grepioni, Crystal Engineering with Hydrogen Bonds, in *Encyclopedia of Supramolecular Chemistry*, eds. J. L. Atwood and J. W. Steed, Marcel Dekker, Inc., New York; Basel, 2004, vol. 1, A-Min.
16. G. R. Desiraju, *Angew. Chem., Int. Ed.*, 2007, **46**.
17. G. R. Desiraju, Review of General Principles, in *Comprehensive Supramolecular Chemistry*, eds. D. D. MacNichol, F. Toda and R. Bishop, Pergamon, Oxford, 1996, vol. 6, pp. 4-9.

18. G. R. Desiraju, Hydrogen Bonding, in *Encyclopedia of Supramolecular Chemistry*, eds. J. L. Atwood and J. W. Steed, Marcel Dekker, Inc. , New York; Basel, 2004, vol. 1, pp. 658-665.
19. G. R. Desiraju and T. Steiner, *The Weak Hydrogen Bond In Structural Chemistry and Biology*, Oxford University Press, 2006.
20. T. Steiner, *Angew. Chem., Int. Ed.*, 2002, **41**, 48-76.
21. T. Steiner and G. R. Desiraju, *Chem. Commun.*, 1998, 891-892.
22. D. V. Soldatov and I. S. Terekhova, *J. Struct. Chem.*, 2005, **46**, S1-S8.
23. T. L. Threlfall, *Analyst*, 1995, **120**, 2435-2460.
24. I. Dance, π-π Interactions: Theory and Scope, in *Encyclopedia of Supramolecular Chemistry*, eds. J. L. Atwood and J. W. Steed, Marcel Dekker, Inc., New York; Basel, 2004.
25. H.-J. Schneider, van der Waals Forces, in *Encyclopedia of Supramolecular Chemistry*, eds. J. L. Atwood and J. W. Steed, Marcel Dekker, Inc., New York; Basel, 2004.
26. B. Sarma, L. S. Reddy and A. Nangia, *Cryst. Growth Des.*, 2008, **8**, 4546-4552.
27. T. J. Mooibroek, P. Gamez and J. Reedijk, *CrystEngComm*, 2008, **10**, 1501-1515.
28. T. R. Shattock, K. K. Arora, P. Vishweshwar and M. J. Zaworotko, *Cryst. Growth Des.*, 2008, **8**, 4533-4545.
29. F. Wöhler, *Annalen*, 1844, **51**.
30. A. D. Bond, *CrystEngComm*, 2007, **9**, 833-834.
31. G. R. Desiraju, *CrystEngComm*, 2003, **5**, 466-467.
32. J. D. Dunitz, *CrystEngComm*, 2003, **5**, 506-506.
33. N. Shan and M. Zaworotko, *Drug Discovery Today*, 2008, **13**, 440-446.
34. M. C. Etter, *Acc. Chem. Res.*, 1990, **23**, 120-126.
35. C. B. Aakeröy, M. E. Fasulo and J. Desper, *Mol. Pharmaceutics*, 2007, **4**, 317-322.
36. P. Vishweshwar, J. A. McMahon and M. J. Zaworotko, Crystal Engineering of Pharmaceutical Co-crystals, in *Frontiers in Crystal Engineering*, eds. E. R. T. Tiekink and J. J. Vittal, John Wiley & Sons, Ltd, 2006, pp. 25-49.
37. M. L. Peterson, M. B. Hickey, M. J. Zaworotko and O. Almarsson, *J. Pharm. Pharmaceut. Sci.*, 2006, **9**, 317-326.
38. A. V. Trask, *Mol. Pharmaceutics*, 2007, **4**, 301-309.
39. E. Mitscherlich, *Ann. Chim. Phys.*, 1822, **19**, 350-419.
40. G. R. Desiraju, *Cryst. Growth Des.*, 2008, **8**, 3-5.

41. P. Vishweshwar, J. A. McMahon, J. A. Bis and M. J. Zaworotko, *J. Pharma. Sci.*, 2006, **95**, 499-516.
42. W. C. McCrone, *Physics and Chemistry of the Solid State*, Interscience, New York, 1965.
43. M. C. Etter, J. C. Macdonald and J. Bernstein, *Acta Crystallogr., Sect. B*, 1990, **46**, 256-262.
44. W. Clegg, A. J. Blake, R. O. Gould and P. Main, *Crystal Structure Analysis Principles and Practice*, International Union of Crystallography, Oxford University Press, 2001.
45. N. Takata, K. Shiraki, R. Takano, Y. Hayashi and K. Terada, *Cryst. Growth Des.*, 2008, **8**, 3032-3037.
46. N. Rodríguez-Hornedo, S. J. Nehm, K. F. Seefeldt, Y. Pagán-Torres and C. J. Falkiewicz, *Mol. Pharmaceutics*, 2006, **3**, 362-367.
47. X.-F. Wang, Y.-B. Zhang, H. Huang, J.-P. Zhang and X.-M. Chen, *Cryst. Growth Des.*, 2008, **8**, 4559-4563.
48. D. Braga, S. L. Giaffreda, F. Grepioni, A. Pettersen, L. Maini, M. Curzi and M. Polito, *Dalton Trans.*, 2006, 1249-1263.
49. A. V. Trask, N. Shan, W. D. S. Motherwell, W. Jones, S. H. Feng, R. B. H. Tan and K. J. Carpenter, *Chem. Commun.*, 2005, 880-882.
50. K. Chadwick, R. Davey and W. Cross, *CrystEngComm*, 2007, **9**, 732-634.
51. A. V. Trask, D. A. Haynes, W. D. S. Motherwell and W. Jones, *Chem. Commun.*, 2006, 51-53.
52. C. Aakeröy, J. Desper, M. Fasulo, I. Hussain, B. Levin and N. Schultheiss, *CrystEngComm*, 2008, **10**, 1816-1821.
53. C. B. Aakeröy and D. J. Salmon, *CrystEngComm*, 2005, **7**, 439-448.
54. J. A. Bis, P. Vishweshwar, D. Weyna and M. J. Zaworotko, *Mol. Pharmaceutics*, 2007, **4**, 401-416.
55. H. J. S. Machado and A. Hinchliffe, *J. Mol.Struct. (Theochem)*, 1995, **339**, 255-258.

CHAPTER 2

Experimental and analytical techniques

2.1 CO-CRYSTAL STARTING MATERIALS

All compounds were supplied by Sigma-Aldrich and used without further purification. A summary of the co-crystal formers used is found in Table 2.1.The crystal structures of each of these starting materials are discussed in the relevant chapters. Solvents used include methanol (MeOH), ethanol (EtOH), acetonitrile (CH_3CN), ethyl acetate (EtOAc), isopropyl alcohol (IPA), acetone, and distilled water (H_2O), all of which were used as supplied.

Table 2.1 Physical properties of the starting materials used in co-crystallisation experiments.

Co-crystal former	Molecular formula	M_r / g mol^{-1}	mp / °C	Physical appearance (description)	Density* / g cm^{-3}
Catechol (O2)	$C_6H_6O_2$	110.11	100-103	white block crystals	1.419 (100 K)
Resorcinol (O3)	$C_6H_6O_2$	110.11	110-113	white crystals	1.311(120 K)
Hydroquinone (O4)					
***α*–form**	$C_6H_6O_2$	110.11	172-175	white crystals	1.378 (173 K)
***β*–form**	$C_6H_6O_2$	110.11	172-175	white crystals	1.258 (293-303 K)
***γ*–form**	$C_6H_6O_2$	110.11	172-175	white crystals	1.381 (283-303 K)
Pyridazine (N2)	$C_4H_4N_2$	80.09	-8	yellow oil	1.346 (100 K)
Pyrimidine (N3)	$C_4H_4N_2$	80.09	19-22	colourless crystals	1.320 (107 K)
Pyrazine (N4)	$C_4H_4N_2$	80.09	50-56	white crystals	1.306 (184 K)
Phthalazine (BN2)	$C_8H_6N_2$	130.15	89-92	yellow needles	1.328 (100 K)
Quinazoline (BN3)	$C_8H_6N_2$	130.15	46-48	yellow crystals	1.322 (295 K)
Quinoxaline (BN4)	$C_8H_6N_2$	130.15	29-32	light yellow crystals	1.362 (120 K)

*Density obtained from crystal structures in the CSD[1], apart from phthalazine. Temperatures of data collection are stipulated in brackets.

2.2 CRYSTAL GROWTH

In general, crystals were obtained *via* slow solvent evaporation, adaptations to this method are discussed in the appropriate sections. The general procedure was as follows: the relevant compounds were dissolved in a minimum amount of a suitable solvent and subjected to sonication to ensure complete dissolution. Some samples were subjected to a short period of heating using a heat gun if the solutes were not completely dissolved after sonication. The individual procedures for each of the co-crystal products are discussed below.

GRID 1: Benzenediol and diazine isomers

β–O2N2 (1:2)

To catechol (64 mg, 0.6 mmol) were added pyridazine (64 mg, 0.8 mmol) and a small quantity of acetone. Slow evaporation of the solvent at ca 4 °C afforded colourless plates of β–O2N2.

O2N3 (1:1):

To catechol (64 mg, 0.6 mmol) were added pyrimidine (64 mg, 0.8 mmol) and a small quantity of acetone. The solvent was left to evaporate slowly at ca 4 °C to afford colourless blocks of O2N3.

O2N4 (2:1):

To catechol (64 mg, 0.6 mmol) were added pyrazine (64 mg, 0.8 mmol) and a small quantity of acetone. Slow evaporation of the solvent at ca 4 °C afforded colourless rods of O2N4.

O3N2 (1:1):

To resorcinol (64 mg, 0.58 mmol) were added pyridazine (64 mg, 0.80 mmol) and a minimum of a 1:1 methanol/water solution. Slow solvent evaporation at room temperature afforded colourless shards of O3N2 in an oily orange residue.

α–O3N3 (1:1):

To resorcinol (64 mg, 0.6 mmol) were added pyrimidine (64 mg, 0.8 mmol) and a minimal quantity of acetone. Slow evaporation of the solvent at ca 4 °C afforded colourless plates of α–O3N3.

β–O3N3 (2:1):

Approximately stoichiometric amounts of resorcinol (64 mg, 0.6 mmol) and pyrimidine (64 mg, 0.8 mmol) were ground with a mortar and pestle for approximately 5 min after addition of 3 drops of methanol. The solid material obtained was used as seeding material for a methanolic solution of the same components. Slow evaporation of the solvent afforded colourless rods of β–O3N3.

***α*–O3N4 (1:1):**

To resorcinol (64 mg, 0.6 mmol) were added pyrazine (64 mg, 0.8 mmol) and a minimum of acetonitrile. The solvent was left to evaporate slowly to dryness affording colourless plates of *α*–O3N4.

***β*–O3N4 (3:1):**

To resorcinol (64 mg, 0.6 mmol) were added pyrazine (64 mg, 0.8 mmol) and a minimum of acetonitrile. The solvent was then allowed to evaporate slowly to dryness to afford colourless plates of *β*–O3N4.

***α*–O4N2 (1:1):**

To hydroquinone (88 mg, 0.8 mmol) were added pyridazine (80 mg, 1.0 mmol) and a small quantity of acetonitrile. Slow solvent evaporation in the absence of light afforded colourless plates of *α*–O4N2.

***β*–O4N2 (1:2):**

To hydroquinone (88 mg, 0.8 mmol) were added pyridazine (80 mg, 1.0 mmol) and a minimum of acetonitrile. Slow solvent evaporation in the absence of light afforded colourless blocks of *β*–O4N2.

O4N3 (1:1):

To hydroquinone (88 mg, 0.8 mmol) were added pyrimidine (80 mg, 1.0mmol) and a minimum of acetonitrile. Solvent was left to evaporate slowly to dryness in the absence of light to afford colourless blocks of O4N3.

O4N4 (1:1):

To hydroquinone (88 mg, 0.8 mmol) were added pyrazine (80 mg, 1.0 mmol) and a small quantity of methanol. Slow solvent evaporation afforded colourless blocks of O4N4.

GRID 2: Benzenediol and benzodiazine isomers

O2BN23 (1:2):

To catechol (11 mg, 0.1 mmol) were added phthalazine (15.6 mg, 0.12 mmol) and a minimum of acetonitrile. Slow solvent evaporation at room temperature afforded orange plates of O2BN23.

O4BN23 (1:2):

To hydroquinone (11 mg, 0.1 mmol) were added phthalazine (15.6 mg, 0.12 mmol) and a minimum of acetonitrile. Solvent was left to evaporate slowly to dryness at room temperature yielding yellowish plates of O4BN23.

O2BN3 (1:1)

An approximate 1:2 molar ratio of catechol (22mg, 0.2 mmol) and quinoxaline (64 mg, 0.5 mmol) was ground for 10 min on the lowest speed setting in a mechanical mill after addition of 3 drops of methanol. The solid product was rinsed into a glass vial with ethanol and the solvent was allowed to evaporate slowly at room temperature to yield yellow rod crystals of the 1:1 O2BN3.

O3BN4 (1:2):

To resorcinol (11 mg, 0.1 mmol) were added quinoxaline (15.6 mg, 0.12 mmol) and a minimum of acetonitrile. Slow solvent evaporation at room temperature afforded yellow blocks of O3BN4.

***α*–O4BN3 (1:2)**

An approximate 1:2.5 molar ratio of hydroquinone (22 mg, 0.2 mmol) and quinazoline (64 mg, 0.5 mmol) were ground for 10 min on the lowest speed setting in a mechanical mill after addition of 3 drops of methanol. A small sample of the ground material was dissolved in ethanol and allowed to evaporate to dryness to afford colourless blocks of *α*–O4BN3.

***β*–O4BN3 (1.6:1)**

An approximate 1.6:1 molar ratio of hydroquinone (67.7 mg, 0.6 mmol) and quinazoline (50 mg, 0.4 mmol) were ground for 10 min on the lowest speed setting in a mechanical mill after addition of 3 drops of methanol. The resulting solid product was dissolved in ethanol and transferred to a glass vial from which the solvent was allowed to evaporate to dryness at room temperature, yielding colourless blocks of *β*–O4BN3.

O2BN4 (1:1 - ASU):

An approximate 1:2.5 molar ratio of catechol (22 mg, 0.2 mmol) and quinoxaline (64 mg 0.5 mmol) were ground for 10 min on the lowest speed setting in a mechanical mill after addition of 3 drops of methanol. A small sample of the ground material was dissolved in

ethanol and the solvent was allowed to evaporate to dryness to afford yellow rods of a 1:1 O2BN4.

2.3 PREPARATION BY SOLVENT–DROP GRINDING (SDG)

Solvent-drop grinding experiments were carried out manually with an Agate mortar and pestle or mechanically using an in-house modified jigsaw (Makita, 50-60 Hz/500-3100 strokes per min. (SPM)) instrument. The sample holder used for the mechanical grinding is an approximately 5 cm long stainless steel capsule with a 5 mm diameter stainless steel ball for grinding. Typically, the two sample components are loaded into the stainless steel capsule together with a few drops of solvent and the steel ball, and the capsule is then fastened into a bracket attached to the jigsaw blade.

After preliminary grinding experiments, a general protocol was formulated in which samples were pulverized for 10 min at the lowest speed setting (500 SPM). The milled material was then scraped from the walls of the capsule and stored in a glass vial for further analysis. Residual material was washed from the stainless steel cylinder into a glass vial with ethanol that was then allowed to evaporate slowly with the expectation of forming suitable single crystals for SCD analysis.

2.4 THERMAL ANALYSIS

Differential Scanning Calorimetry is used to determine the difference in heat flow between a sample and a reference material (most often an empty pan), that are subjected to the same thermal program.[2] Differences in temperature between the sample and reference infers that a thermal event has taken place; these events can be related to glass transitions, phase transitions (changes in heat capacity, solid-solid transition, eutectics, melting, sublimation *etc*.). DSC is used in this study to determine the onset temperature of a melt or phase transition. DSC is used in conjunction with PXRD to verify the preparation of a novel co-crystal phase.

Differential Scanning Calorimetry (DSC) was carried out using a TA Instruments Q100 system under a N_2 gas purge (flow rate of 50.0 ml/min) coupled to a cooling unit. A standard procedure was established and used for all compounds. Starting at an initial temperature of 20 °C, the sample was cooled to -20.0 °C at a set ramp rate (either 2.5, 5 or 10 °C min^{-1}), maintained at this temperature for 1 min, then ramped to approximately 10 °C above the melting point of the higher melting starting material, and then cooled back down to 20 °C. The procedure was subsequently repeated such that each sample completes two thermal

cycles per run. A 5 °C min^{-1} ramp rate was typically chosen for analysis with 2.5 °C min^{-1} and 10 °C min^{-1} ramp rates used to corroborate the results obtained.

Sample preparation was minimal in all cases: a powdered sample of approximately 5-10 mg was placed in an aluminium pan which was non-hermetically sealed with vented aluminium lids. Reference pans were prepared in a similar manner.

2.5 SOLUTION NMR

Synthesised ligands and intermediate products (Chapter 5) were characterised using ^{1}H and ^{13}C NMR experiments. These were performed on either a Varian Unity Inova 400 MHz NMR spectrometer or a 300 MHz Varian VNMRS NMR spectrometer. All spectra were collected at room temperature using standard procedures.

2.6 SINGLE-CRYSTAL DIFFRACTION (SCD) AND ANALYSIS

The determination of a material's single crystal structure is arguably the most definitive of all characterising techniques available today. SCD is a non-destructive technique that utilises X-ray radiation to ultimately determine the atomic coordinates of a molecule(s) in the solid-state. Solid-state materials yield characteristic diffraction patterns with reflection intensities for the constituting atoms and analysis of these parameters allows a 3-D structure determination from which vital information concerning chemical formula, bond lengths and angles as well as absolute configuration can be elucidated.

In all cases crystals were immersed in paratone oil and a suitable crystal selected and mounted onto a MiTeGen mount that was then placed onto the goniometer head of the Single Crystal Diffractometer for data collection. X-ray intensity data were collected on a Bruker-Nonius SMART Apex diffractometer equipped with a fine-focus sealed tube and a 0.5 mm Monocap collimator (monochromated Mo-Kα radiation, $\lambda = 0.71073$ Å). Data were captured with a CCD (Charge-Coupled Device) area-detector with the generator powered at 40 kV and 30 mA. A constant stream of nitrogen gas is produced by an Oxford Cryogenics Cryostat (700 Series Cryostream Plus) coupled to the diffractometer for low temperature (100 K) data collection of all structures. On occasion crystals would deteriorate rapidly on removal from this nitrogen stream.

SMART[3] software was employed to implement an appropriate data collection strategy after a reliable unit cell had been determined. Standard ω-scans were used to obtain intensity data which were subsequently reduced and refined using SAINT[4] software. A multi-scan absorption correction was performed utilising SADABS.[5] All structures were solved by

direct methods using SHELXS-97.[6] SHELXL-97 was employed within the X-Seed[7,8] environment to refine the resulting structure by full matrix least-squares based on F^2. Thermal parameters, bond angles and hydrogen bonding patterns were used to distinguish between carbon and nitrogen atoms and all non-hydrogen atoms were refined anisotropically. Owing to the characteristics of the hydrogen atom (discussed in Chapter 1, Section 1.3.1), hydrogen atoms of the aromatic rings are placed using a riding model constraint (*mn* = 43) based on idealized coordinates and geometrical constraints.[9] The distance constraint for an aromatic C–H interaction is given as 0.93 Å and increased by 0.02 Å to compensate for the low temperature data collection so that bond lengths are 0.95 Å. Hydroxyl hydrogen atoms were located in Fourier difference maps and refined isotropically. Disordered structure refinement is discussed in the relevant sections (Chapter 3, Section 3.2.6).

2.7 POWDER X-RAY DIFFRACTION (PXRD)

Powder diffraction analysis is another non-destructive technique used primarily to characterise solid materials. It is an especially useful tool in monitoring structural changes that may take place in the solid state. It can also be useful in the verification of the composition of a bulk sample from which a single crystal structure has been selected. This method is becoming more extensively used in a high-throughput analysis of compounds under investigation, particularly in the pharmaceutical industry, where time and money are of the essence.

The powder diffractometer that was utilised for this study is a Bruker D8 ADVANCE model with Bragg-Brentano geometry using Cu Kα radiation (λ = 1.5406 Å) generated at 40 kV and 30 mA and diffracted from the sample onto a Dynamic scintillation (point-type) detector for data capture.

All samples were prepared in the same manner – gentle grinding with a mortar and pestle followed by sample loading into a standard sample holder or mounted onto a glass slide if there was insufficient sample to fill the holder. A general operating procedure was used for all samples – samples were scanned from 4–40° 2θ at increments of 0.04° with 2 s scan steps. Data were collected at a constant room temperature of 22 °C.

A number of aspects of PXRD need to be taken into account when analysing diffractograms – sample preparation is important to ensure uniform particle size to maximise precision of the data collection and to ensure high resolution in the resulting diffraction pattern. The phenomenon of preferred orientation can also affect the results such that some

peaks are more intense relative to others in the pattern. To counteract this, samples are generally rotated at a constant speed throughout data collection. However, samples in this study were not rotated since peaks below 5° 2θ would be obscured by the lip of the sample holder when rotated, and the pattern obtained would be incomplete. When comparing experimental data with a pattern simulated from single-crystal data, the temperature at which the data is collected should be taken into account and any deviations justified. In this study all PXRD diffractograms were acquired at 22 °C (295.2 K) and all SCD structural data were collected at 100 K (-173.2 °C). Therefore, all predicted patterns are generally shifted slightly to the right assuming positive thermal expansion along all axes at the elevated temperature. This is owing to the inverse relationship between *d* and °2θ in Bragg's Law:

$$n\lambda = 2d\sin\theta,$$

where λ is the incident radiation wavelength, *d* is the reciprocal lattice spacing and θ is the angle of the incident X-ray beam

A decrease in temperature would bring about a contraction of the crystal's unit cell dimensions, which are coupled to the *d* spacings within the crystal lattice. These, in turn, are inversely related to the angles measured in the diffraction pattern (2θ), thus explaining why the predicted pattern (collected at lower temperature) would be shifted slightly to the right.

2.8 COMPUTER PACKAGES

- **CAMBRIDGE STRUCTURAL DATABASE (CSD)**

The Cambridge Structural Database[1] (CSD) is a structural resource that allows one to search published single crystal as well as powder structural data using a single convenient interface. Restrictions (limits) can be imposed on the search in order to refine the data search. As of 1 January 2009, 201 606 organic molecules and 248 408 inorganic structures have been deposited in the CSD. A wealth of knowledge can be obtained from a statistical analysis of compounds already present in the CSD, including understanding the nature of certain bond types (especially hydrogen bonds) and other intermolecular interactions and can be used in the identification of frequently occurring patterns and supramolecular synthons.[10] The **Mercury**[11] and **Vista** interfaces were also used to visually analyse the structures and compare the statistical data retrieved respectively.

- **CRYSTAL EXPLORER**

Crystal Explorer[12] is a computer package that utilizes calculated Hirshfeld surfaces[13] of molecules within a crystal structure to determine the intermolecular interactions between particular molecules or for the crystal structure in its entirety. Hirshfeld surfaces are created by an extension of the weight function describing an atom in a molecule, to include the function of a molecule in a crystal.[14] The isosurface generated from these calculations, with a specified weight function $w(r) = 0.5$, surrounds the molecule and by partitioning the electron density of the molecular fragments, delineates the space occupied by a molecule in a crystal.[14] Hirshfeld surfaces can provide information about intermolecular interactions in the crystal as the surface is determined by both the enclosed molecule and its closest neighbours.[14] Other molecular surfaces used to visualise and quantify molecular geometries such as the fused sphere van der Waals (or CPK) and smoothed Connelly surfaces do not have this advantage as they are designated only by the molecule itself.[14] For quality data regarding intermolecular interactions to be extracted from Hirshfeld surfaces, the only prerequisite is that the crystal structures imported into the program are well-characterised with all hydrogen atoms located accurately.

The equation used to define a Hirshfeld surface is w(r) = 0.5 where w(r) is the weight function described as

$$w(r) = \sum_{i \in molecule} \rho_i(r) / \sum_{i \in crystal} \rho_i(r);$$

where $\rho_i(r)$ is a spherical atomic electron distribution located at the i^{th} nucleus.

The surfaces incorporated in this study are all calculated using the d_{norm} function[15] so that the contact distance is normalised according to the formula

$$d_{norm} = \frac{d_i - r_i^{vdW}}{r_i^{vdW}} + \frac{d_e - r_e^{vdW}}{r_e^{vdW}},$$

d_i is the distance from the surface to the nearest atom interior to the surface; d_e is the distance from the surface to the nearest atom exterior to the surface (Figure 2.1). The sum of the two distances would give an approximate contact distance.

Surfaces generated are depicted using a sliding colour scheme (Figure 2.2), with contacts closer than the sum of their van der Waals radii highlighted in red, longer contacts in blue, while contacts approximately equal to the sum of van der Waals radii are white.

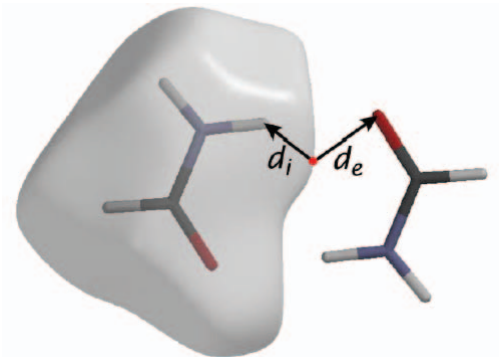

Figure 2.1 Definition of the d_i and d_e distances in establishing the Hirshfeld surface.[15]

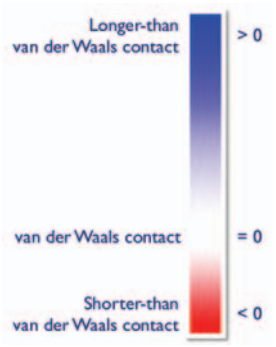

Figure 2.2 The sliding colour scale of d_{norm} Hirshfeld surfaces taken from the Crystal Explorer online manual.[14]

A 2-D fingerprint plot combining the d_i and d_e distances is a more visual representation of the relationship between these descriptors.[14] The d_i, d_e pairs are binned in intervals of 0.01 Å and the colouring of each bin in the 2-D histogram is a function of the fraction of surface points in that bin. The sliding colour scale from blue (few points) through green to red (many points) indicates the concentration of points in each bin. Fingerprint plots (Figure 2.) provide a means of rapid comparison of two or more crystal structures by virtue of the fact that each plot is unique to a crystal structure and is highly sensitive to a molecule's immediate environment.[14] A number of interaction types have distinctive shapes in the 2-D plot that can be used to quickly identify these interactions in the crystal structure. Specific interactions can be highlighted in the plot by selecting the relevant atom types, these areas are shaded blue, while the remainder of the interactions are grey. The interactions highlighted in Figure 2.3 are the most significant to this particular study and will be referred to in the descriptions of the structures reported.

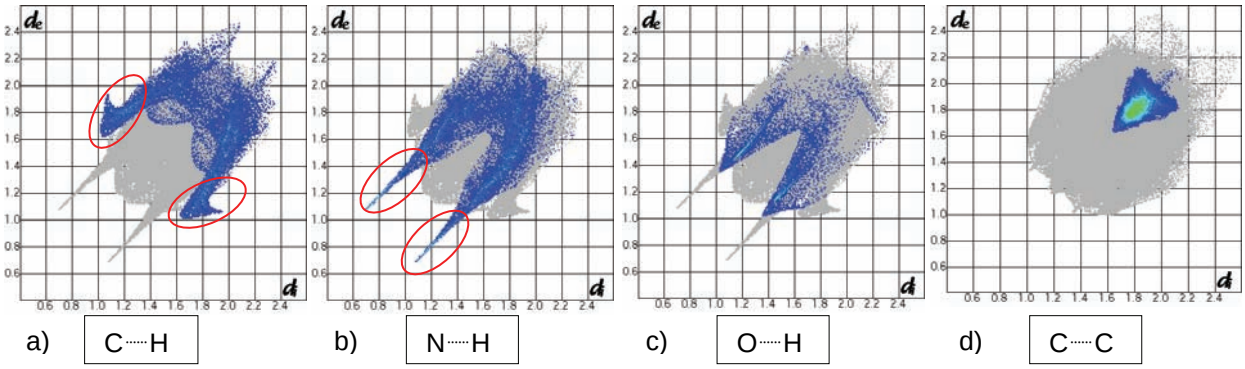

Figure 2.3 Selected characteristic patterns for symmetry–related interactions between molecules interior and exterior to the Hirshfeld surface. The blue areas highlight the specific interaction, while the grey areas represent the remainder of the intermolecular interactions. In each interaction type there are characteristic markers that can be identified. a)'Wings' represent C····H interactions most often as C–H····π interactions, b) the outer tails are indicative of N····H interactions, c) O····H interactions are represented by inner tails, and d) the concentrated green area on the diagonal is indicative of C····C interactions, most often π····π type.[16]

- **SAINT+**[4] was used to convert raw crystallographic frame data to a set of integrated intensities with standard deviations, direction cosines, and XYZ centroids. This is achieved by an integration method similar to that reported by Kabsch,[17] using 3-D profiling algorithms.
- **SADABS**[5,18] (Siemens Area Detector Absorption Corrections) is an application in the APEX suite used to scale and correct data collected on a Bruker AXS area detector utilising .raw files generated by SAINT+
- **XPREP**[19] (Reciprocal Space Exploration) was used to determine crystal symmetry and space groups for single-crystal data by the analysis and manipulation of intensity data. Input files can be uncorrected .raw files obtained directly from SAINT+ or scaled .hkl files from SADABS.
- **X-Seed**[7,8] is a graphical software program used as an interface for the SHELX-97 software suite used to solve and refine single-crystal data from .ins files (generated by XPREP) and the reflection files (.hkl) obtained from SADABS. X-seed also provides a platform for generating structural images using POV-RAY. Structures retrieved from the CSD can also be imported into X-Seed for packing analysis.
- Structural images were rendered using **POV-RAY**[20] (Persistence of Vision Raytracer)

2.9 CHEMICAL MODELLING

Theoretical modelling was performed by Dr Catharine Esterhuysen, and a summary of the results is included in the relevant sections. For calculations performed for comparison of stabilisation energies of structures *α*–O4N2 and *β*–O4N2, the positions of the hydroxyl hydrogen atoms in models, comprised of four molecules of hydroquinone and four or eight

molecules of pyridazine, were optimised using density functional theory (DFT) at the B971 level of theory, utilising the 6-31G(d) basis set. Interaction energies between pairs of molecules were calculated by determining the difference in energies between single point calculations of the dimer at the B971/6-311G(d) level of theory, with the Counterpoise correction and those of the individual molecules involved in the interaction.

For energy comparisons of Scenarios 1 & 2 of the crystal structure of O4N3, the positions of the hydroxyl hydrogen atoms in models containing one molecule each of hydroquinone and pyrimidine were optimised at the B971 level of theory, utilising the 6-31G(d) basis set. Interaction energies between pairs of molecules were calculated by determining the difference in energies between single point calculations of the dimer at the B971/6-311G(d) level of theory, with the Counterpoise correction, and those of the individual molecules involved in the interaction.

REFERENCES

1. F. Allen, *Acta Crystallogr., Sect. B*, 2002, **58**, 380-388.
2. M. A. White, Thermal Analysis and Calorimetry Methods, in *Comprehensive Supramolecular Chemistry*, eds. J. E. D. Davies and J. A. Ripmeester, Pergamon, Oxford, 1996, vol. 8, pp. 179-197.
3. *SMART*, Bruker, 2002.
4. *SAINT*, Bruker, 2003.
5. R. Blessing, *Acta Crystallogr., Sect. A*, 1995, **51**, 33-38.
6. G. M. Sheldrick, *Acta Crystallogr., Sect. A*, 2008, **64**, 112-122.
7. L. J. Barbour, *J. Supramol. Chem.*, 2001, **1**, 189-191.
8. J. L. Atwood and L. J. Barbour, *Cryst. Growth Des.*, 2003, **3**, 3-8.
9. G. M. Sheldrick, *SHELX Manual*, http://shelx.uni-ac.gwdg.de/SHELX/shelx.pdf.
10. A. Nangia, *CrystEngComm*, 2002, **4**, 93-101.
11. C. F. Macrae, P. R. Edgington, P. McCabe, E. Pidcock, G. P. Shields, R. Taylor, M. Towler and J. van de Streek, *J. Appl. Cryst.*, 2006, **39**, 453-457.
12. S. K. Wolff, D. J. Grimwood, J. J. McKinnon, D. Jayatilaka and M. A. Spackman, *Crystal Explorer 2.1 (381)*, University of Western Australia, Perth, 2007.
13. F. L. Hirshfeld, *Theor. Chim. Acta*, 1977, **44**, 129-138.
14. M. A. Spackman and D. Jayatilaka, *CrystEngComm*, 2009, **11**, 19-32.
15. *The Crystal Explorer Manual*, http://hirshfeldsurface.net/wiki/index.php/Surface_Properties, Accessed 15 Dec 2008.

16. M. A. Spackman and J. J. McKinnon, *CrystEngComm*, 2002, 378-392.
17. W. Kabsch, *J. Appl. Cryst.*, 1988, **21**, 67-72.
18. G. M. Sheldrick, University of Göttingen, Germany, 2002.
19. *XPREP - Reciprocal space exploration, Version 6.14 - w95/98/NT/2000/ME*, Bruker Nonius, 2003.
20. *POV-Ray for Windows, Version 3.6.1a.icl8.win32*, Persistence of Vision Team, Persistence of Vision Pty. Ltd. , 2003-2004.